

RESEARCH PAPER

Photocatalytic Dye Degradation Properties of Zinc Copper Ferrites Nanoparticles

Arthur Charles Prabakar¹, Balaraman Sathyaseelan^{2*}, Govindarasu Killivalavan¹, Iruson Baskaran³, Krishnamoorthy Senthilnathan⁴, Elayaperumal Manikandan⁵, Dhananjayan Sivakumar⁶

¹ Research Scholar, Department of physics, Bharathiar University, Coimbatore-641046, India

² Department of Physics, University College of Engineering Arni, Anna University Chennai, Arni 632326, Tamil Nadu, India.

³ Department of Physics Arignar Anna Government Arts College, Cheyyar 604407, Tamil Nadu, India

⁴ Photonics Division, School of Advanced Sciences, VIT University, Vellore, 632014, Tamil Nadu, India

⁵ Department of Physics, Thiruvalluvar University College of Arts and Science, Thennangur Village, Vandavasi Taluk, Tiruvannamalai District 604408, India

⁶ Department of Physics, Sree Krishna College of Engineering, Unai, Anaicut-632101, Tamilnadu, India.

ARTICLE INFO

Article History:

Received 02 July 2019

Accepted 05 September 2019

Published 01 October 2019

Keywords:

Nanocrystalline Materials

Structural

VSM

Zinc Copper Ferrite

ABSTRACT

In the present study, new multi-components spinel ferrite Zinc doped metallic ferrites are investigated. The synthesized compounds consisting of Zinc copper ferrite nanostructures were developed using the Co-precipitation technique. Powder X-ray diffraction pattern (XRD) confirms the formation of the spinel phase for all the samples. The lattice constant was studied through powder X-ray diffraction data analysis. The lattice constant of all Zinc copper ferrite concentration was found to be less than that of bulk values. The chemical composition, surface morphology and crystallinity of the samples have been examined by scanning electron microscopy (SEM) and High-Resolution Transmission Electron Microscope (HRTEM). Besides, selected area electron diffraction (SAED) confirms the evolution of phases and Energy Dispersive X-ray (EDX) respectively. The effect of Zinc copper ferrite nanoparticles, the magnetic properties were investigated by using Vibration Sample Magnetometer (VSM). The obtained hysteresis (M-H) curves of all the samples were analysed under the applied magnetic field of range ± 10 K Oe at room temperature. The magnetic properties such as saturation magnetisation (Ms), remnant magnetization (Mr) and coercivity (Hc) values are calculated. The data obtained from magnetic studies, the variation among the magnetic properties have been investigated for annealed 600 °C sample. The prepared Zinc copper ferrite nanoparticles should be extended to various potential applications, such as photodegradation of methylene blue (MB) dye under visible-light irradiation and results showed that 65% of the dye was degraded. Catalysis, separation, and purification processes.

How to cite this article

CharlesPrabakar A, Sathyaseelan B, Killivalavan G, Baskaran I, Senthilnathan K, Manikandan E, sivakumar D. Photocatalytic Dye Degradation Properties of Zinc Copper Ferrites Nanoparticles. J Nanostruct, 2019; 9(4): 694-701.

DOI: 10.22052/JNS.2019.04.011

INTRODUCTION

Nowadays renewable energy sources are highly explored and preferred by a lot of developing and developed countries in order to minimize the greenhouse gas discharges.[1,2]. Ferrites are iron-containing compounds that are categorized into spinels, hexagonal ferrites and garnets [3]. Nano-structured iron containing transition metal

oxide materials are known to exhibit interesting physical and chemical properties. In addition, these properties are significantly different from those of conventional bulk materials owing to their extremely small size and large surface area. Ferrites of the form MFe_2O_4 (M = Ni²⁺, Co²⁺, Cu²⁺, Zn²⁺, etc.,) have been gaining considerable momentum as they are highly used in the

* Corresponding Author Email: bsseelan03@gmail.com

electronic materials industries. Other transition metal oxides that have been widely investigated are oxides of copper, cobalt and nickel [4]. Fd3m is the space group for the structure of spinel ferrite. The cubic unit cell consists of 56 atoms, 32 oxygen anions which are distributed in a cubic close-packed structure. Here, 24 cations occupy 8 of the 64 available tetrahedral sites (A sites) and 16 of the 32 available octahedral sites (B sites) [5]. The distribution of cation depends on the electronic configuration and valence of ions. The useful properties of ferrite nanoparticles depend on both sizes as well as cation distribution. If the atom size decreases, the surface region increases. It results in improving the catalytic properties [6, 7]. Nevertheless, each nanoparticle can behave as a single magnetic domain. From the literature survey, it was found that changes in the particle size can determine the magnetic properties due to the change in cation distribution [8]. Nanoparticle synthesis of these could be various methods such as sol-gel [9], sol-gel auto-combustion method [10], and co-precipitation method [11]. Moreover, important properties of ferrites are determined by the cation site occupations at the tetrahedral and octahedral sub lattices [12, 13].

In the present work, Aim to study the prepared Zinc copper ferrite nanoparticles by chemical co-precipitation technique. The Characterization of the Structural, morphological and magnetic properties of the Zinc copper ferrite nanoparticles was analysed through powder XRD, TEM and VSM. Furthermore, the Photocatalysis property was also analysed.

MATERIALS AND METHODS

All the chemicals were analytical graded and used without further refining. Typically, the solution of 0.2M Fe (NO₃) 3.9H₂O, 0.08M Zn (NO₃) 2.6H₂O, 0.02M Cu (NO₃) 2.6H₂O and 0.5 g Polyethylene glycol 200 (PEG) were dissolved in distilled water with a constant stirring. The precipitating reagent ammonia hydroxide (25%) was added drop-wise into metal solutions, contained in a beaker, with constant stirring until co-precipitation occurred and the PH reached 10. The reaction temperature was maintained at 85 °C for 45 minute. The final product was dried in an oven at a temperature of 110 °C for 24 hrs to remove water contents and annealing at various temperatures such as 500 and 600°C for 2hrs was carried out.

Characterization studies

The confirmation of spinel phase purity was evaluated by Powder XRD measurement. Morphological features were evaluated by SEM. Morphology, as well as the particle size of the sample, was probed using HRTEM. The photo-degradation experiments for methylene blue (MB) dye molecule over Zinc Copper ferrite, annealed at 600°C, were determined by measuring the absorbance value at approximately 484nm using a Shimadzu UV-2501PC spectrometer. Infrared spectra were obtained using Fourier transform infrared spectroscopy (FT-IR, Nicolet 6700) in the 400 - 4000 cm⁻¹ range. The magnetic properties of these samples were carried out by Vibrating Sample Magnetometer (VSM) (model Lake Shore 7307) with an applied magnetic field range ± 10 KOe at room temperature.

RESULTS AND DISCUSSION

Structural Analysis

The crystalline structure of the Zinc copper ferrite as prepared and annealed at 500°C and 600°C are shown in Fig.1. All of the diffraction peaks can be indexed to the standard Zinc copper ferrite with the cubic spinel structure and the reflection peaks match well with standard data (JCPDS 82-1042). This indicates the synthesized nanoparticles have Fd3m space group and indicating high degree purity. The average crystallite sizes, D, are calculated from the (311) peaks through the Scherrer's formula around 32 nm. It is observed that the sample Zn_{1-x}Cu_xFe₂O₄ crystallized in cubic structure and the lattice parameter is found to be 8.355 Å, which is less than the values reported for bulk compounds. This is mainly because of the replacement of smaller Cu²⁺ ions (0.72 Å) by larger Zn²⁺ ions (0.74 Å) [14,15]. In addition, as the ionic radius of Zn²⁺ is larger than the ionic radius of Cu²⁺, the Zn²⁺ substitution leads to larger expansion of the lattice. Consequently, the lattice parameter increases more when compared to the Cu²⁺ substitution in the synthesized particles. Since ionic radius of Fe²⁺ (0.74 Å) ion is larger than Fe³⁺ ion (0.64 Å), the lattice constant increases [16]. Nonmagnetic transition metal ions Zn²⁺ and Cu²⁺ ion prefer octahedral sites whereas Fe³⁺ ions prefer both tetrahedral and octahedral sites.

Scanning Electron Microscopy (SEM) and Energy dispersive X-Ray spectra (EDX) Analysis

Using the typical SEM analysis, morphological

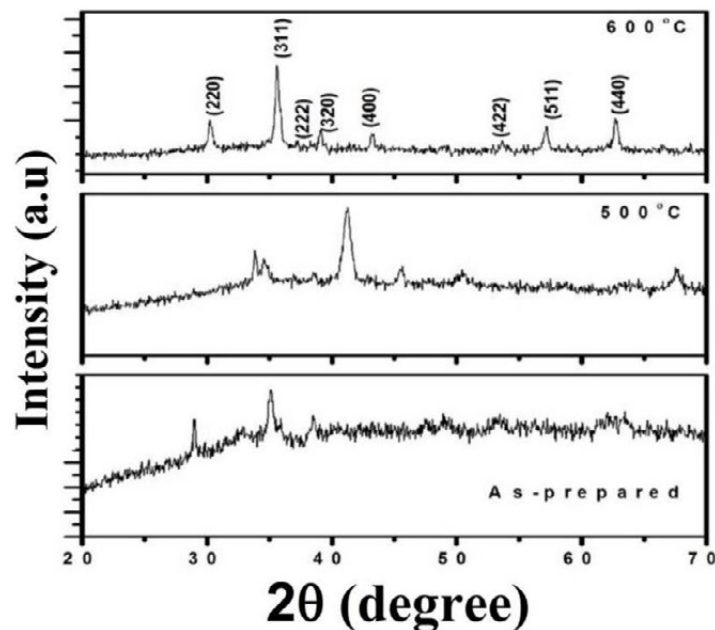


Fig.1. XRD patterns of Zinc copper ferrite nanoparticles as prepared, annealed at 500°C, and 600°C.

characteristics of Zinc copper ferrite nanoparticles annealed at 600°C are shown in Fig.2 (a). They show the formation of multigrain agglomerations consisting of fine crystallites with irregular shapes and sizes. Ferrite powders possessed a coarse structure with crystalline microstructure with an average grain size homogeneous is about 50 μm obtained from SEM images. This is larger than size of nanocrystals calculated using the XRD measurements, which, in turn, simply indicates that each grain is formed by aggregation of a larger number of nanocrystals. The samples are irregular shapes and sizes, and cohesion of grains is due to the magnetic attraction. A drastic difference in microstructure of the annealed at 600°C products indicated that the substitution to the metal ions like Zn, and Cu surface of these microstructure. EDX analysis confirms the stoichiometric proportion of Zinc copper ferrite nanoparticles annealed at 600°C and also the percentage proportion of the constituent elements is shown in Fig.2 (b). The elemental weight proportion percentage is presented in the tables of weight and atomic percentage proportions, the constituent elemental proportion and the ratios are in line with expected elemental proportion and the oxygen (O) and iron (Fe) being with highest peaks in all of the samples [17]. Typical EDX analysis reveals the existence of elements of Zn, Cu, Fe, and O.

High Resolution Transmission Electron Microscopy Analysis (HRTEM)

As portrayed in Fig.3 (a), HRTEM micrographs also confirm the particle size of Zinc copper ferrite nanoparticles annealed at 600°C. The average crystallite size is around 8.38 nm. HRTEM analysis reveals that the particles are nearly spherical in shape. The average crystallite size estimated from HRTEM image is found to be in good agreement with the observed values from powder XRD results. From Fig.3 (b), HRTEM image of individual Zinc copper ferrite nanocrystal indicates that the interplanar distance is 0.26. In the SAED (Fig.3(c)) image of annealed at 600°C Zinc copper ferrite nanoparticles, the diffraction rings match well with standards powder XRD diffraction data that confirms good crystallinity. The observed crystallographic d values of 2.52 Å correspond to the lattice space of (311) plane of the Zinc copper ferrite system. The observed crystallographic d values agree well with those obtained from powder XRD analysis.

Fourier transform infrared spectroscopy (FT-IR) Studies

FT-IR spectra are usually assigned to the vibration of ions in the crystal lattice, which can be used to confirm the positions of Zn^{2+} , Cu^{2+} , and Fe^{3+} ions in spinel structure. The vibrating sample

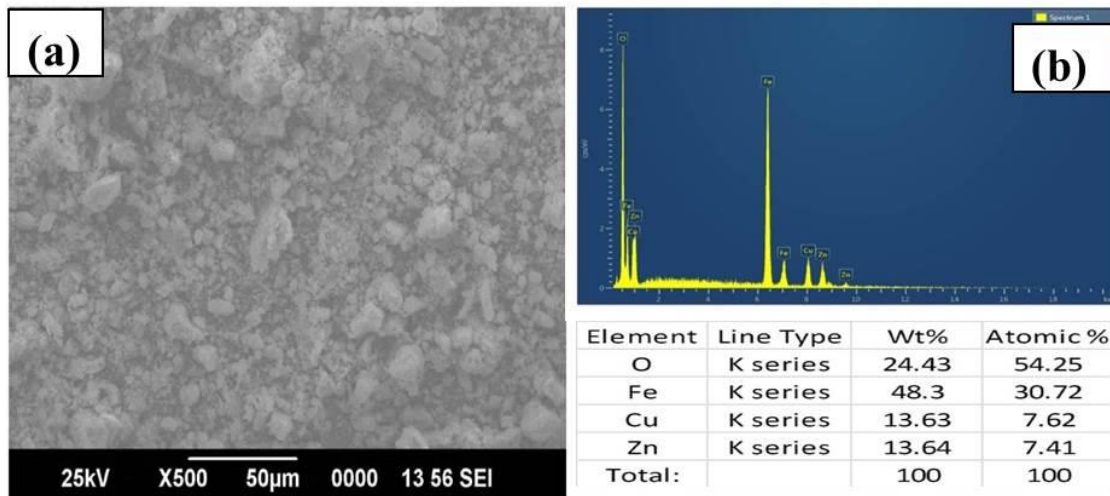


Fig.2. Images of Zinc copper ferrite nanoparticles annealed at 600°C (a) SEM (b) EDX analysis.

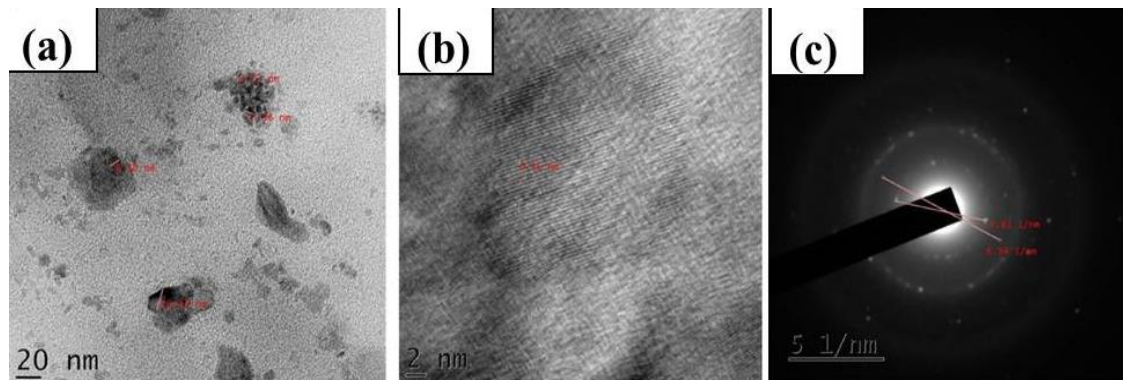


Fig.3. Image of Zinc copper ferrites nanoparticles annealed at 600°C, (a) HRTEM (b) Inter planar distance (c) SAED

magnetometer is used to measure the magnetic properties of samples.

Fig. 4 shows the typical FT-IR spectra of Zinc copper ferrite nanoparticles recorded between 4000 and 400 cm^{-1} . In the range of 1000 - 400 cm^{-1} , The two main absorption bands at 522 and 862 cm^{-1} correspond to the Fe-O bonds in the tetrahedral and octahedral sites, respectively, confirming the spinel structure of Fe_3O_4 nanoparticles. Similar results are observed in Zinc copper ferrite nanoparticles prepared by sol-gel combustion method [18-21]. When Zn^{2+} ions are replaced by Cu^{2+} ions, due to charge imbalance some Fe^{3+} ions shift from A sites to B sites, making the $\text{Fe}^{3+}\text{-O}^{2-}$ stretching vibration in greater. So the decrease in peak intensity of ν_1 with increasing Cu^{2+} content is mainly attributed to the change in $\text{Fe}^{3+}\text{-O}^{2-}$ bands. The broad peaks that appear from 3205 to 2978 cm^{-1} and the IR absorption peaks between 1350 and 1066 cm^{-1} are due to

the fundamental and overtones O-H stretching vibrations of the hydroxyl groups of water on the nanoparticles, respectively [22]. These results are consistent with the previous reports [23, 24]

Magnetic Properties

Fig. 5 shows a typical hysteresis loop of all the Zinc copper ferrite nanoparticles compositions which are annealed at 600°C. By using a vibrating sample magnetometer, the measurements of magnetisation for all the compositions were carried out under the applied magnetic field of range $\pm 10\text{k Oe}$ at room temperature. It is observed that, the magnetic properties such as saturation magnetisation ($M_s=16.184 \text{ emu/g}$), remnant magnetisation ($M_r=0.38935 \text{ emu/g}$) and coercivity ($H_c=23.875 \text{ G}$) values in good agreement with the literature values [25].

The magnetic structure of spinel ferrite is ferrimagnetic, the magnetic moments of A and B

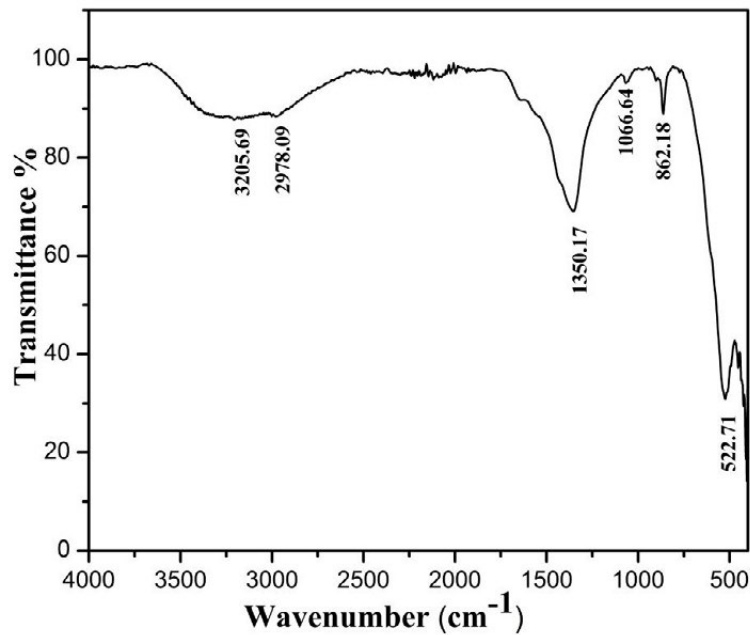


Fig.4. FT-IR spectra of Zinc copper ferrite nanoparticles.

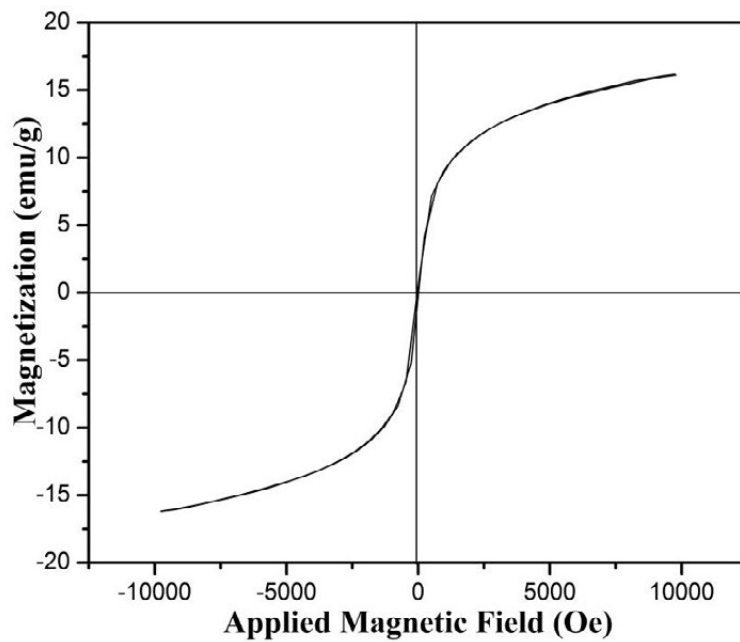


Fig.5. Magnetic hysteresis loops for Zinc copper ferrite nanoparticles annealed sample at 600°C.

sites are coupled antiparallel to each other. There are twice as many B sites filled, so there is a net magnetic moment equal to the difference between the two sites. The magnetization behaviour of spinel ferrite can be understood in Neel's model [26, 27]. Zinc-copper ferrite nanoparticles of the composition and cation distribution among the A and B sites will influence the magnetic properties

of samples.

According to this, in any ferrite, the magnetic order of tetrahedral clusters (A-site) and octahedral clusters (B-site) was found to be antiparallel to each other. In this, the A-A and B-B superexchange interaction was predominated by A-B super exchange interaction.

According to Neel's model, the net magnetic

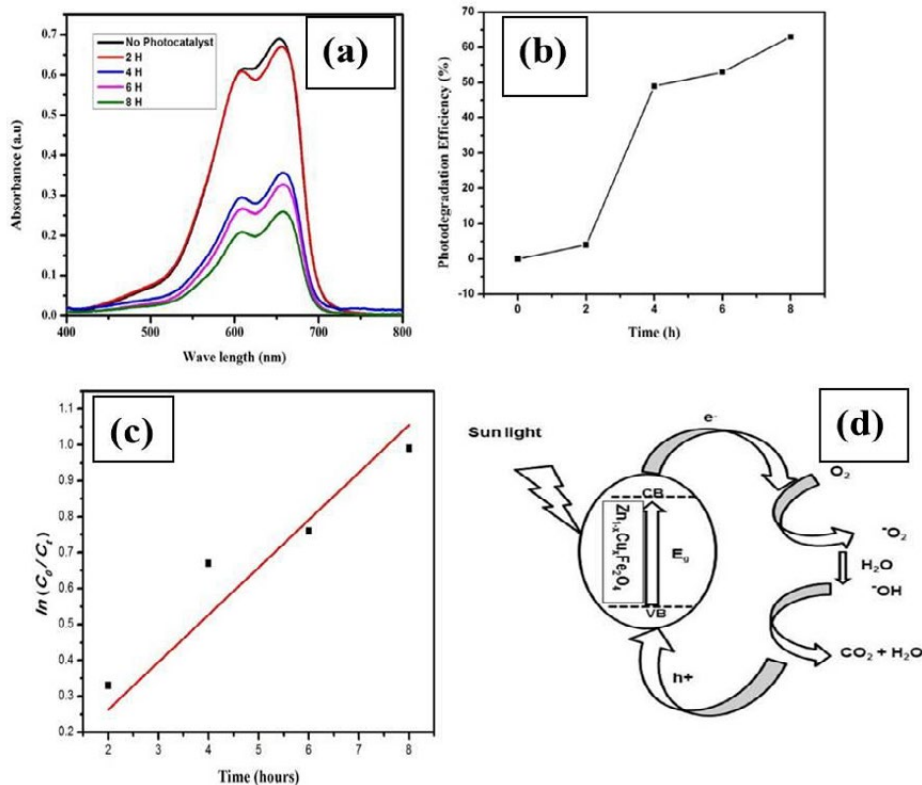


Fig.6. Zinc copper ferrite nanoparticles annealed at 600°C under UV-light irradiation (a) Absorption of MB solution during the photo-degradation (b) Photo-degradation percentage (c) Plots of $\ln(C_0/C_t)$ versus irradiation time (d) Photocatalytic mechanism of MB in catalyst.

moment of the composition per formula is expressed as:

$$\mu_B = M_B(x) - M_A(x)$$

where M_B and M_A are the magnetic moments of B and A sub lattices respectively.

Squareness ratio or remnant ratio ($M_r/M_s=0.024$) of a material is one of the important characteristics which depends on its anisotropy. The values of the squareness ratio represent the random arrangement of uniaxial particles along with the cubic magnetocrystalline anisotropy [28,29].

In the present work, the squareness ratio of Zinc copper ferrite nanoparticles is 0.024 at room temperature. And it has been observed from the literature that the squareness, which indicates the presence of non-interacting single domain particles with cubic anisotropy in the respective compositions [30]. The values of Bohr Magneton (μ_B) of these samples were also evaluated by using the following Equation (3).

$$\mu_B = M_s M_w / 5585$$

where: M_w is the molecular weight of the sample; M_s is saturation magnetisation.

$$5585 = \beta \times N \quad [\beta \text{ is Conversion factor } (9.27 \times 10^{-21}); N \text{ is Avogadro's number}].$$

It is observed that Bohr Magneton values are 1.56. With the research interest, one can modify the compositions of ferrite materials in accordance with squareness ratio (S), for the development of new electromagnetic materials [26]. In the present work, it is observed a clear variation on magnetic properties of Zinc copper ferrite nanoparticles.

Photocatalytic Degradation

The photo-degradation of methylene blue by Zinc copper ferrite nanoparticles is evaluated and the observed absorption spectra are presented in Fig.6 (a). It is clearly shown in the figure that the characteristic absorption peak of the methylene blue (MB) at about 664 nm decreases gradually with increasing exposure time from 0 to 8 hours and almost disappears after 8 hours of irradiation time. This indicates that the MB dye has almost degraded. The photocatalytic performance of the

NPs is observed by plotted (C/Co) as a function of time for MB dye and the same is shown in Fig. 6 (b). The presence of Zinc copper ferrite nanocrystal implies the good photo-degradation activity for MB, and no obvious degradation of dye molecules was observed in the darkness, especially, the degradation percentage of MB after 8 hrs. However, Zinc copper ferrite sample exhibited 65%. The dependence of MB photo-degradation on the crystallite size of Zinc copper ferrite nanocrystals is shown in Fig.6 (c). Further, it illustrates that the degradation percentage of MB and their kinetics [31, 32]. Photocatalytic reaction mechanisms for oxidation of MB dye by Zinc copper ferrite are presented in Fig.6 (d). Photocatalytic activities have been improved by Zinc copper ferrite and it can be ascribed from the photo absorptions spreading even up to the visible region and minimizing the electron-hole recombination rate.

CONCLUSION

Zinc-copper ferrite nanoparticles were prepared through a chemical co-precipitation technique. Structural analysis through powder X-ray diffractometry confirms the spinel phase of all the prepared compounds. TEM also confirms the particle agglomeration and a crystallite size is in agreement with the XRD results. It is observed that the magnetic properties M_s , M_r , and H_c . The squareness ratio (S) the existence of non-conducting domain particles is in accordance with the ions concentration. The obtained Bohr Magneton (μ_B) values also follow the ions concentration. The synthesized ferrite powder exhibited a good response towards photocatalytic activity for the degradation of MB under visible light irradiation. The optimum conversion achieved was 65%.

CONFLICT OF INTEREST

The authors declare that there is no conflict of interests regarding the publication of this manuscript.

REFERENCES

- Athanas AK, McCormick N. Clean energy that safeguards ecosystems and livelihoods: Integrated assessments to unleash full sustainable potential for renewable energy. *Renewable Energy*. 2013;49:25-8.
- Hinrichs-Rahlwes R. Renewable energy: Paving the way towards sustainable energy security. *Renewable Energy*. 2013;49:10-4.
- Saleh H.I. Synthesis and Formation Mechanisms of Calcium Ferrite compounds. *J. Mater. Sci. Technol*, 2004; 20(5): 530-534.
- Rezlescu N, Rezlescu E, Tudorache F, Popa P. D. *Romanian Reports in Physics*. 2009; 61: 223-234.
- Carta D, Casula MF, Falqui A, Loche D, Mountjoy G, Sangregorio C, et al. A Structural and Magnetic Investigation of the Inversion Degree in Ferrite Nanocrystals MFe_2O_4 (M = Mn, Co, Ni). *The Journal of Physical Chemistry C*. 2009;113(20):8606-15.
- Fan G, Gu Z, Yang L, Li F. Nanocrystalline zinc ferrite photocatalysts formed using the colloid mill and hydrothermal technique. *Chemical Engineering Journal*. 2009;155(1-2):534-41.
- Qiu J, Wang C, Gu M. Photocatalytic properties and optical absorption of zinc ferrite nanometer films. *Materials Science and Engineering: B*. 2004;112(1):1-4.
- Tang ZX, Sorensen CM, Klabunde KJ, Hadjipanayis GC. Size-dependent Curie temperature in nanoscale $MnFe_2O_4$ particles. *Physical Review Letters*. 1991;67(25):3602-5.
- Zahi S, Hashim M, Daud AR. Preparation of Ni-Zn-Cu ferrite particles by sol-gel technique. *Materials Letters*. 2006;60(23):2803-6.
- Azadmanjiri J, Salehani HK, Barati MR, Farzan F. Preparation and electromagnetic properties of $Ni_{1-x}Cu_xFe_2O_4$ nanoparticle ferrites by sol-gel auto-combustion method. *Materials Letters*. 2007;61(1):84-7.
- Shi Y, Ding J, Liu X, Wang J. $NiFe_2O_4$ ultrafine particles prepared by co-precipitation/mechanical alloying. *Journal of Magnetism and Magnetic Materials*. 1999;205(2-3):249-54.
- Sulaiman NH, Ghazali MJ, Majlis BY, Yunas J, Razali M. Superparamagnetic calcium ferrite nanoparticles synthesized using a simple sol-gel method for targeted drug delivery. *Bio-Medical Materials and Engineering*. 2015;26(s1):S103-S10.
- D S, K CBN, K PN, M MR, G Rk, B S, et al. Structural Characterization and Dielectric Studies of Superparamagnetic Iron Oxide Nanoparticles. *Journal of the Korean Ceramic Society*. 2018;55(3):230-8.
- Tan X, Li G, Zhao Y, Hu C. The effect of Cu content on the structure of $Ni_{1-x}Cu_xFe_2O_4$ spinels. *Materials Research Bulletin*. 2009;44(12):2160-8.
- Zhang H.E, Zhang B.F, Wang G.F, Dong X.H, Gao Y. The structure and magnetic properties of $Ni_{1-x}Zn_xFe_2O_4$ ferrite nanoparticles prepared by sol-gel auto-combustion. *J. Magn. Mater*, 2007; 312: 126-130.
- Denton AR, Ashcroft NW. Vegard's law. *Physical Review A*. 1991;43(6):3161-4.
- Kim WC, Kim SJ, Lee SW, Kim CS. Growth of ultrafine $NiZnCu$ ferrite and magnetic properties by a sol-gel method. *Journal of Magnetism and Magnetic Materials*. 2001;226-230:1418-20.
- Tan X, Li G, Zhao Y, Hu C. The effect of Cu content on the structure of $Ni_{1-x}Cu_xFe_2O_4$ spinels. *Materials Research Bulletin*. 2009;44(12):2160-8.
- Xiang J, Shen X, Song F, Liu M. One-dimensional $NiCuZn$ ferrite nanostructures: Fabrication, structure, and magnetic properties. *Journal of Solid State Chemistry*. 2010;183(6):1239-44.
- Umare SS, Ningthoujam RS, Sharma SJ, Shrivastava S, Kurian S, Gajbhiye NS. Mössbauer and magnetic studies on nanocrystalline $NiFe_2O_4$ particles prepared by ethylene

- glycol route. *Hyperfine Interactions*. 2008;184(1-3):235-43.
21. Rais A, Taibi K, Addou A, Zanoun A, Al-Douri Y. Copper substitution effect on the structural properties of nickel ferrites. *Ceramics International*. 2014;40(9):14413-9.
 22. Fajaro F, Setyawan H, Widiyastuti W, Winardi S. Synthesis of magnetite nanoparticles by surfactant-free electrochemical method in an aqueous system. *Advanced Powder Technology*. 2012;23(3):328-33.
 23. Lu W, Shen Y, Xie A, Zhang W. Green synthesis and characterization of superparamagnetic Fe₃O₄ nanoparticles. *Journal of Magnetism and Magnetic Materials*. 2010;322(13):1828-33.
 24. Deligöz H, Baykal A, Şenel M, Sözeri H, Karaoğlu E, Toprak MS. Synthesis and characterization of poly(1-vinyltriazole)-grafted superparamagnetic iron oxide nanoparticles. *Synthetic Metals*. 2012;162(7-8):590-7.
 25. Maaz K, Mumtaz A, Hasanain SK, Ceylan A. Synthesis and magnetic properties of cobalt ferrite (CoFe₂O₄) nanoparticles prepared by wet chemical route. *Journal of Magnetism and Magnetic Materials*. 2007;308(2):289-95.
 26. Bhukal S, Namgyal T, Mor S, Bansal S, Singhal S. Structural, electrical, optical and magnetic properties of chromium substituted Co–Zn nanoferrites Co_{0.6}Zn_{0.4}CrxFe_{2-x}O₄ (0x1.0) prepared via sol–gel auto-combustion method. *Journal of Molecular Structure*. 2012;1012:162-7.
 27. Smart JS. The Néel Theory of Ferrimagnetism. *American Journal of Physics*. 1955;23(6):356-70.
 28. Raut AV, Barkule RS, Shengule DR, Jadhav KM. Synthesis, structural investigation and magnetic properties of Zn²⁺ substituted cobalt ferrite nanoparticles prepared by the sol–gel auto-combustion technique. *Journal of Magnetism and Magnetic Materials*. 2014;358-359:87-92.
 29. Berkowitz, A.E. and Kneller, E. *Magnetism and Metallurgy*. 1654; Vol.1:Academic Press, New York, 295.
 30. Ibusuki T, Kojima S, Kitakami O, Shimada Y. Magnetic anisotropy and behaviors of Fe nanoparticles. *IEEE Transactions on Magnetics*. 2001;37(4):2223-5.
 31. Ramaswamy V, Jagtap NB, Vijayanand S, Bhang DS, Awati PS. Photocatalytic decomposition of methylene blue on nanocrystalline titania prepared by different methods. *Materials Research Bulletin*. 2008;43(5):1145-52.
 32. Syoufian A, Nakashima K. Degradation of methylene blue in aqueous dispersion of hollow titania photocatalyst: Optimization of reaction by peroxydisulfate electron scavenger. *Journal of Colloid and Interface Science*. 2007;313(1):213-8.